15th World Congress on Computational Mechanics (WCCM-XV)
8th Asian Pacific Congress on Computational Mechanics (APCOM-VIII)
Virtual Congress: 31 July – 5 August 2022
S. Koshizuka (Ed.)

CONSTRUCTING MACHINE-LEARNED INTERATOMIC POTENTIALS FOR COVALENT BONDING MATERIALS AND MD ANALYSES OF DISLOCATION AND SURFACE

JUNYA MORIGUCHI[1], KEN-ICHI SAITOH[2], KENJI NISHIMURA[3],

TOMOHIRO SATO[2], MASANORI TAKUMA[2], AND YOSHIMASA TAKAHASHI[2]

[1]Graduate School, Kansai University
3-3-35 Yamate-cho Suita-shi Osaka 564-8680 Japan
k020516@kansai- u.ac.jp

[2] Faculty of Engineering Science
Kansai University

[3] National Institute of Advanced Industrial Science and Technology

Key words: Silicon, Silicon carbide, Machine learning, Molecular dynamics, Density functional theory, Interatomic potential, Mechanical properties, Genetic algorithm

Abstract. *As machine learning potentials for molecular dynamics (MD) simulations, Spectral Neighbor Analysis Potential (SNAP) and quadratic SNAP (qSNAP) were constructed for silicon (Si) and silicon carbide (SiC). The reproducibility of the basic material properties about perfect crystal, free surface and dislocation cores in Si and 3C-SiC was investigated. The coefficients of SNAP and qSNAP were optimized using liner regression to present energy and force obtained by DFT. In addition, hyperparameters (cutoff length and weights for optimization, here) were determined using genetic algorithm to reproduce elastic moduli obtained by DFT. Lattice constant and elastic moduli of Si crystal by MD using our SNAP or qSNAP agree well with the values of DFT, and they have higher accuracy than those by any empirical potential. Additionally, melting point and specific heat at constant pressure were calculated by MD correctly. Especially in qSNAP of Si, the surface energy of {100} and {111} planes and the reconstructed {100} surface structure were almost reproduced. For 3C-SiC, SNAP reproduces lattice constant and elastic moduli of DFT. Furthermore, edge dislocation cores were generated successfully. However, the potentials we constructed have insufficient reproducibility in the plastic region, so it is necessary to continue development.*

1 INTRODUCTION

Machine learning (ML) methods have been used in various fields along with the development of digital technology. For example, ML has achieved great results in medical and business fields. In atomistic simulations, ML is expected to be utilized for constructing interatomic potential. Interatomic potential is an essential part of molecular simulations such as molecular dynamics, where mathematical formulation (interatomic potential function) is configured based on some physical model. Therefore, interatomic potential function must be the basis of physical reliability of MD simulation, and is greatly involved in the reproducibility of simulation results. Generally, first, a functional form is determined, and secondly the parameters needed there are fitted so as to reproduce physical properties of the specified material. These procedures are cumbersome especially when the material is relatively unknown with less information of experimental or chemistry data. Theoretically, *ab initio* (first principle) calculations can be applied to obtain unknown properties of any material, but utilizing such method in every atomistic simulation will be too expensive to conduct. It is advantageous to construct in advance some function form together with parameters suitable for the specified material, and then to conduct MD simulations. In this context, ML potentials, which will be automatically constructed only by using *ab initio* data such as those from density functional theory (DFT) simulation, are supposed to be very hopeful. Such ML methods will have general function forms and a large number of parameters, and they can be made to reproduce results in DFT calculations.

Although many types of ML potential have been devised (such as GAP[1], ANN[2]), we focused on Spectral Neighbor Analysis Potential (SNAP)[3]. There is an attempt of calculating the lattice constant and elastic moduli of Si using SNAP and comparing them by other potentials. However, the reproducibility of the surface and dislocations has not been confirmed sufficiently. Therefore, we built from scratch ML potentials for Si and 3C-SiC (covalent bonding materials), and confirmed their reproducibility through MD calculations.

2 METHODS

2.1 Spectral Neighbor Analysis Potential (SNAP)

SNAP is one of the ML potential types[3]. In SNAP, the energy of each atom is expressed by a linear combination of invariant under rotation, which is called a bispectrum $\boldsymbol{B}_i$ and is obtained directly from the atomic configuration and the atomic density around the atom i. The atomic energy is expressed as,

$$E_i = \beta_0 + \sum_{k=1}^{K} \beta_k B_k = \beta_0 + \boldsymbol{\beta} \cdot \boldsymbol{B}_i \,, \tag{1}$$

$$K = \frac{(J_{max}+1)\left(J_{max}+\frac{3}{2}\right)(J_{max}+2)}{3}, \tag{2}$$

where β_0 and β_k are coefficients which are to be fitted to input data in ML process. J_{max} is an adjustable parameter to determine how many components of bispectrum are summed up.

There is an advanced type of SNAP which is called quadratic SNAP (qSNAP)[4]. In qSNAP,

a many-body effect around each atom is considered like in embedded atom method (EAM) potential function. The expressions of qSNAP are,

$$E_i = \boldsymbol{\beta} \cdot \boldsymbol{B_i} + F(\rho_i), \tag{3}$$

$$\rho_i = \boldsymbol{\alpha} \cdot \boldsymbol{B_i}, \tag{4}$$

where $F(\rho_i)$ represents the energy in embedding atom i into the electron density contributed by its neighboring atoms. In EAM, ρ_i is written simply as a sum of pairwise contributions, but in qSNAP it is written as a linear function of bispectrum components and the expression is a little complicated.

2.1 Optimization

For optimization process of ML potentials, we made use of a framework and source codes in an open software, Materials Virtual Lab[5]. For actual calculations, we utilize DAKOTA software[6] as an optimization tool.

In the present study, two crystalline materials, monoatomic silicon (Si) and cubic silicon-carbide (3C-SiC) are focused on. Training data for Si are made by VASP[7] which is one of *ab initio* simulation packages. Those data contain results of self-consistent field (scf) calculation of the crystal structure which is strained or with reconstructed surfaces. It also includes results of *ab initio* MD performed in room (standard) or high temperature. It is effective to augment input by many atomic configurations in finite temperature which are provided by *ab initio* MD. After all, the number of training data used for Si system becomes 214. Training data for 3C-SiC are made by QuantumEspresso (QE)[8] instead, which is also one of *ab initio* simulation packages. Those data contain results of scf calculation for the structure which is strained and results of *ab initio* MD in room (standard) or high temperature. Unfortunately, for SiC, any ab initio result as for free surfaces is not included. After all, the number of training data used for 3C-SiC is 700. We recognize the amount of training data used here are sufficient to construct the SNAP or qSNAP potential[9].

In constructing the SNAP potential, we optimized SNAP coefficient with liner regression for reproducing energy and force by DFT. On the other hand, hyperparameters (cutoff length, and weights for optimization, here) were judged to be optimized by genetic algorithm (GA) when the minimum error in elastic moduli was obtained.

3 RESULTS

3.1 Calculating properties in Si crystal

By using SNAP and qSNAP constructed for Si by us, we calculated lattice constant a_0 (for the cubic lattice of diamond structure) and elastic moduli (C_{11}, C_{12}, C_{44}) as shown in Table 1. The deviations of our calculated values from those of VASP are also written with parentheses in the table. The values by "Analytical Bond-Order Potential (ABOP)[10]" which is an empirical potential are also included for comparison. It is realized that SNAP reproduces VASP and ABOP up to almost the same level. In the case of qSNAP, it has higher accuracy than SNAP and ABOP, especially for elastic moduli.

Table 1: Material constants for Si obtained by ab initio and potentials

		unit	DFT (VASP)	ABOP[10]	SNAP	qSNAP
Lattice constant a_0		Å	5.469	5.429 (0.73%)	5.434 (0.64%)	5.518 (0.9%)
Elastic moduli	C_{11}	GPa	156	169.3 (8.5%)	134.6 (14%)	153.3 (1.7%)
	C_{12}		65	64.14 (1.3%)	73.49 (13%)	65.65 (1.0%)
	C_{44}		76	60.14 (21%)	93.87 (1.2%)	73.69 (3.0%)
Bulk modulus		GPa	95	99.21(4.4%)	93.87 (1.2%)	94.87 (0.14%)

As dynamic properties, calculated specific heat at constant pressure C_p and melting point T_m are considered and the results are shown in Table 2. These calculated values were obtained by heating MD simulations under NPT-ensemble. In estimating C_p, the linear relation between total energy and temperature could be assumed. The melting points could be detected by sudden and large change of system volume under constant pressure, so inevitably the moment of melting become a little ambiguous. These simulations were performed with a periodic structure of perfect crystal of Si, and therefore the calculated melting point is expected to be higher than the experimental value. For ABOP, extraordinarily high melting point was estimated, but, for SNAP and qSNAP, calculated values are in the range of the experiment and seem more correct.

Table 2: Results of heating calculations

		unit	Experiment[11]	ABOP	SNAP	qSNAP
Specific heat at constant pressure	C_p	$\times 10^{-23}$ J/K	5.52	5.20	5.00	5.19
Melting point	T_m	K	1410	3000 ~ 4200	1400 ~ 2100	1700 ~ 2400

3.2 Reproducibility for the structure of Si {100} surface

For the structures with free surface, {100} or {111} plane, we calculated surface energy γ_{100}, γ_{111} and their atomic configuration in the surface. Calculated surface energies are shown in Table 3, and visualized atomic structures of the surface {100} are shown in Figure 1. For the surface {111}, the surface energy is calculated correctly by all potentials. For the surface {100}, qSNAP reproduced the surface energy of VASP well. Besides, since atoms on the top surface form dimer structures, qSNAP could almost reproduce surface reconstruction. To the contrary, ABOP (empirical one) couldn't exhibit any surface reconstruction, because it is formulated with angular dependency of bonds and therefore it does not present specialized bonding state at the surface.

Table 3: Surface energies in Si

	unit	Experiment[12),(13)]	VASP	SNAP	qSNAP	ABOP
γ_{100}	J/m^2	2.13	1.28	0.9877	1.329	1.909
γ_{111}		1.24	1.15	1.285	1.088	0.9963

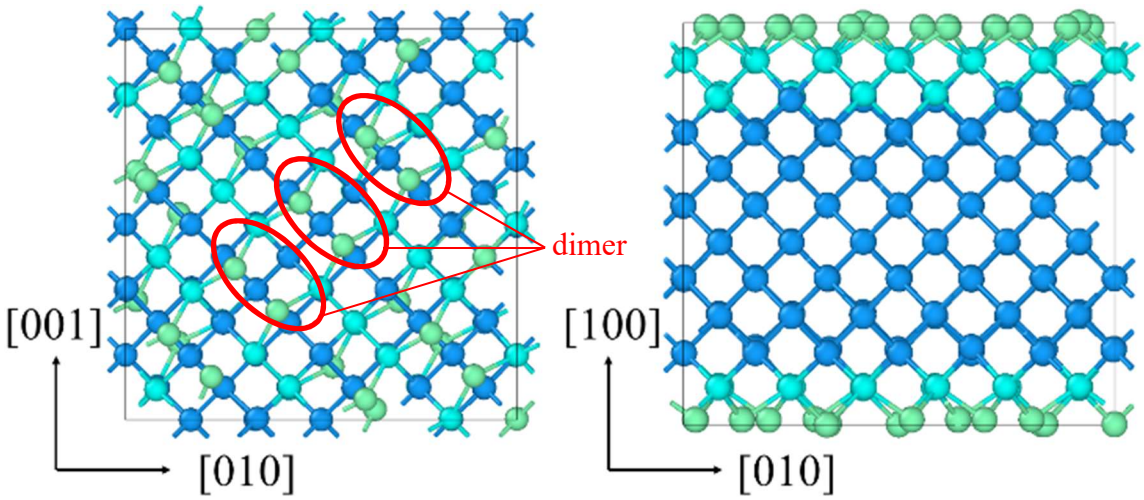

Figure 1: Structure of surface {100} obtained by qSNAP

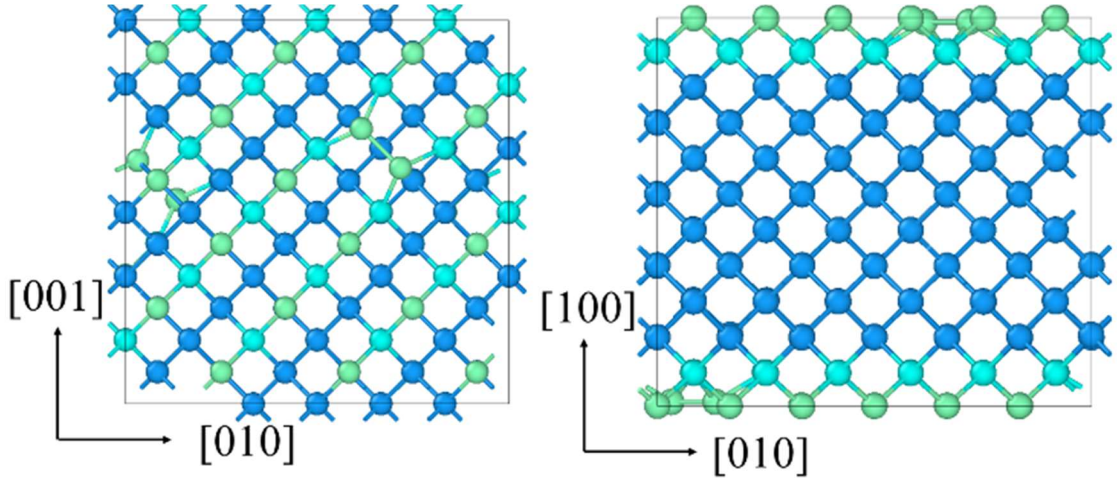

Figure 2: Structure of surface {100} obtained by ABOP (Blue-colored atoms have all of its first and second nearest neighbors positioned on cubic diamond lattice sites. Light blue-colored atoms are the first neighbor of atoms that were classified as cubic diamond. Its four neighbors are positioned on lattice sites, but at least one of its second nearest neighbors is not. Green-colored atoms are the second nearest neighbor of atoms that were classified as cubic diamond. The atom itself is positioned on a lattice site, but at least one of its neighbors is missing or is not positioned on a lattice site.)

3.3 Calculating properties in 3C-SiC

For 3C-SiC crystal, likewise Si, we calculated lattice constant and elastic moduli as shown in Table 4. The deviations of the values obtained by SNAP from those by QE are written with parentheses. “Vashishta potential” is another empirical potential for comparison in addition to ABOP. SNAP reproduces material properties calculated with QE well, and has the same degree of precision as empirical potentials.

Table 4: Material constants for 3C-SiC obtained by ab initio and potentials

		unit	DFT (QE)	ABOP	Vashishta potential	SNAP
Lattice constant a_0		Å	4.358	4.359 (0.022%)	4.358 (0%)	4.365 (0.16%)
Elastic moduli	C_{11}	GPa	388.1	382 (1.6%)	390 (0.49%)	349.2 (10%)
	C_{12}		131.8	145 (10%)	142.6 (8.2%)	133.2 (1.1%)
	C_{44}		243.5	240 (1.4%)	191.0 (22%)	234.4 (3.7%)
Bulk modulus		GPa	216.8	224 (3.3%)	225.2 (3.9%)	205.3 (5.3%)

3.4 The stability of dislocation cores in 3C-SiC by SNAP

We checked the stability of edge dislocations in 3C-SiC crystal under shear deformation. The calculation model has dislocation dipole whose Burgers vectors $\boldsymbol{b}$ are $\frac{1}{6}[1,1,\bar{2}]a_0$ and $-\frac{1}{6}[1,1,\bar{2}]a_0$ as shown in Figure 3. Then, shear strain (ε_{xz} component as shown Figure 3) was applied to the calculated model by deforming the whole cell with a constant strain rate. The moving direction of dislocation cores are supposed to be in $\pm x$ direction in this shearing. The calculation conditions are summarized in Table 5.

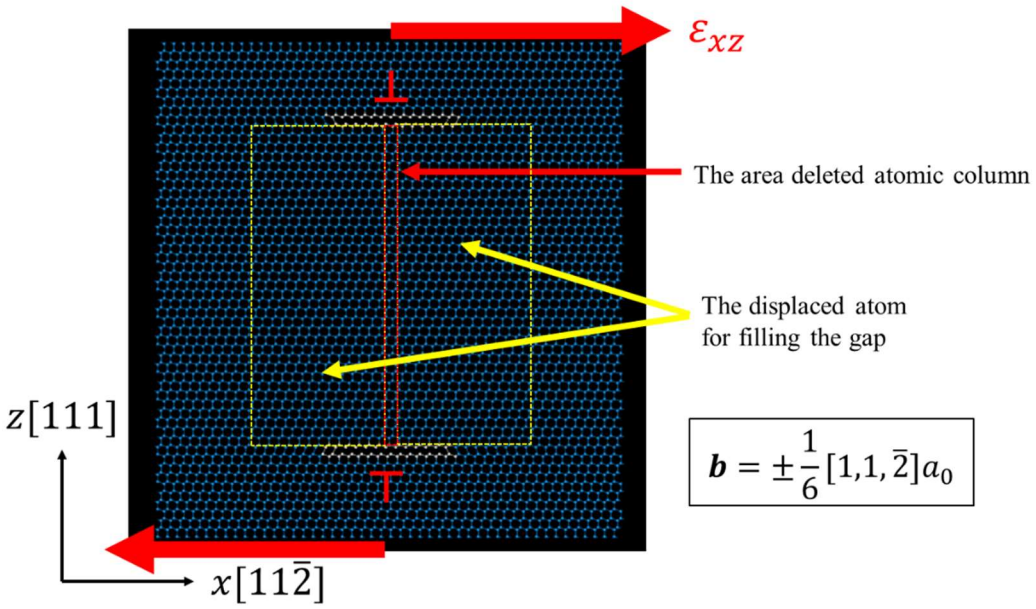

Figure 3: A crystal model including dislocation after deleting atom plane

Table 5: calculate condition in shear deformation

	units	
the number of atoms	-	20448
cell size (x, y, z)	nm	12.70, 1.222, 13.47
temperature T	K	300
Boundary condition	-	periodic (x, y, z)
strain rate	1/s	5.0×10^9
strain type, direction	-	pure shear, xz
time increment Δt	Fs	1.0
simulation time	Ps	10.0

The appearances just after relaxation of dislocation cores and at some moment in shear deformation using SNAP are shown in Figure 4. In those pictures, blue-colored atoms are in perfect crystal (of zinc-blende structure) and white atoms are around lattice defects including dislocation cores. Stress-strain diagram obtained from shear calculation is shown in Figure 5. In ABOP and Vashishta potential, the dislocation core was moving in response to shear deformation. In using SNAP, the crystal structure collapsed from the position of dislocation cores before they started to move. However, elastic modulus C_{44} estimated from the graph of Figure 5 agrees well with the value calculated by *ab initio* method (by QE). Therefore, as for SNAP, the elastic response can be reproduced well in general, but the plastic region is not sufficiently reproduced at the present construction. This is because training data for 3C-SiC

doesn’t contain DFT data concerning plastic region. So, in ML process, adding other data such as for stacking defects is supposed to improve the reproducibility in plastic deformation.

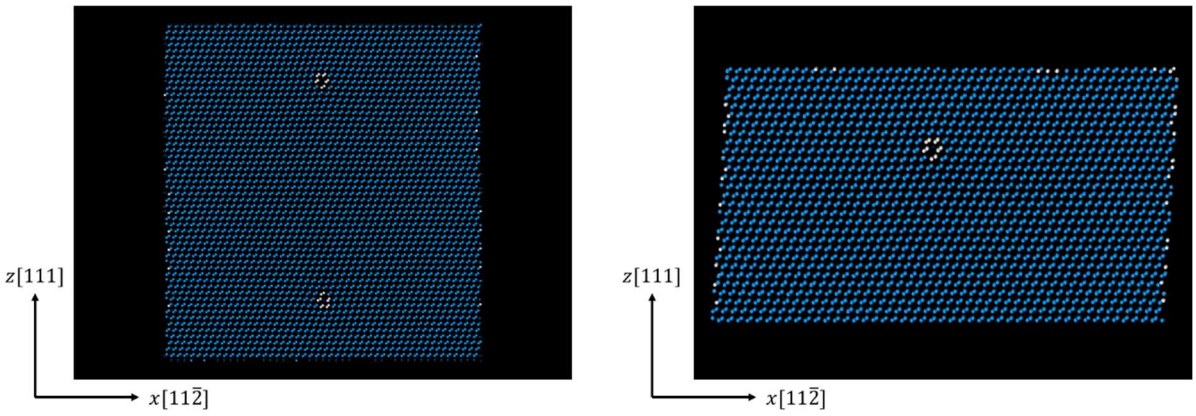

(a) dislocation cores generated after relaxation (b) the structure 3% strain applied (upper half)

Figure 4: Generated dislocation cores and structure after shearing in SNAP

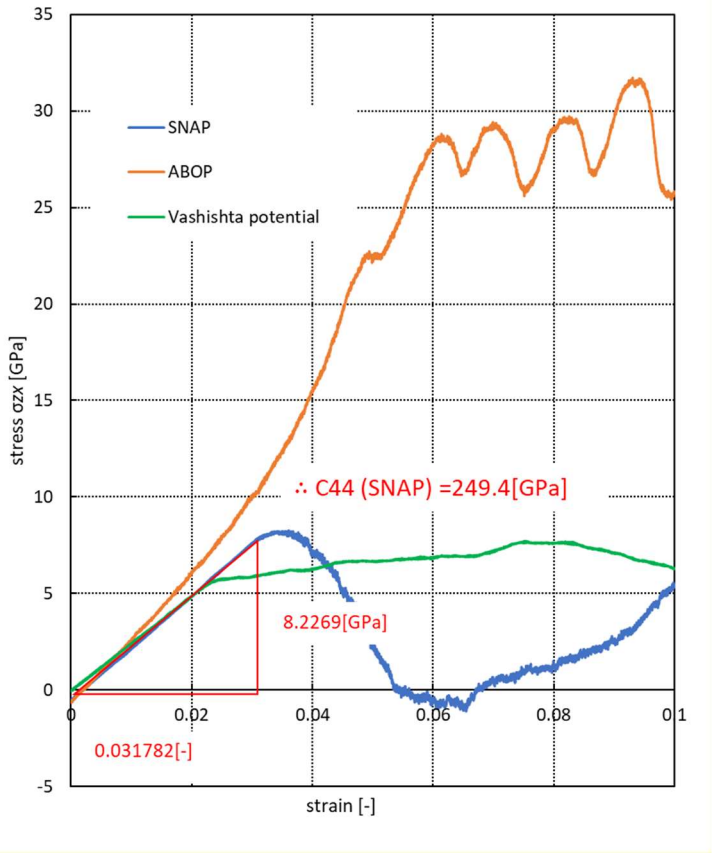

Figure 5: stress-strain diagram obtained from shearing calculation

4 CONCLUSIONS

In this study, we attempted constructing ML potentials for covalent bonding materials.

- SNAP and qSNAP can reproduce basic properties of Si. Besides, the dimer structure in the free surface of Si {100} plane, which has not been predicted by empirical potentials, is successfully obtained by qSNAP.
- The SNAP we built from scratch for 3C-SiC can reproduce lattice constant and elastic moduli. Although the dislocation behavior has not sufficiently been reproduced yet, the improvement is expected by adding other data on stacking defects.

REFERENCES

[1] Szlachta, W.J., Bartok, A.P., and Csányi, G. Accuracy and Transferability of Gaussian Approximation Potential Models for Tungsten. *Phys. Rev. B*: *Condens. Matter Mater. Phys* (2014) **90**:104108.

[2] Artrith, N. and Urban, A. An implementation of artificial neural-network potentials for atomistic materials simulations: Performance for TiO2. *Comput. Mater. Sci*. (2016) **114** :135-150.

[3] Thompson, A.P., Swiler, L.P., Trott, C.R., Foiles, S.M., and Tucker, G.J. Spectral neighbor analysis method for automated generation of quantum-accurate interatomic potentials. *J. Comput. Phys* (2014) **285**:316-330.

[4] Wood, M.A. and Thompson, A.P. Extending the Accuracy of the SNAP Interatomic Potential Form. *J. Chem. Phys* (2018) **148**:1721.

[5] Materials Virtual Lab mlearn URL: https://github.com/materialsvirtuallab/mlearn (accessed 2021-08-02).

[6] DAKOTA URL: https://dakota.sandia.gov/. (accessed 2021-08-02).

[7] VASP URL: https://www.vasp.at/. (accessed 2021-08-02).

[8] QUANTUM ESPRESSO URL: https://www.quantum-espresso.org/. (accessed 2021-08-02).

[9] Zuo, Y., Chen, C., Li, X., Deng, Z., Chen, Y., Behler, J., Csányi, G., Shapeev, A.V., Thompson, A.P., Wood, M.A., and Ong, S.P. Performance and Cost Assessment of Machine Learning Interatomic Potentials. J. Phys. Chem (2020) **124**:731-745.

[10] Erhart, P. and Albe, K. Analytical Potential for Atomistic Simulations of Silicon, Carbon, and Silicon Carbide. *Phys. Rev. B* (2005) **71**:35211.

[11] O'Neil, M.J., Heckelman, P.E., Dobbelaar, P.H., Roman, K.J., Kenny, C.M., Karaffa, L.S. The Merck Index - An Encyclopedia of Chemicals, Drugs, and Biologicals. *Whitehouse Station, NJ: Merck and Co., Inc.* (2006) 1466.

[12] Jaccodine, R.J. Surface Energy of Germanium and Silicon. *J. Electrochem. Soc* (1963) **110**:524.

[13] Gilman, J.J. Direct Measurements of the Surface Energies of Crystals. *J. Appl. Phys* (1960) **31**:2208.